



Contents lists available at ScienceDirect

Biomaterials

journal homepage: [www.elsevier.com/locate/biomaterials](http://www.elsevier.com/locate/biomaterials)

## The *in vivo* degradation of a ruthenium labelled polysaccharide-based hydrogel for bone tissue engineering

Samia Laïb<sup>a</sup>, Borhane H. Fellah<sup>a,b</sup>, Ahmed Fatimi<sup>a</sup>, Sophie Quillard<sup>a</sup>, Claire Vinatier<sup>a</sup>, Olivier Gauthier<sup>a,b</sup>, Pascal Janvier<sup>c</sup>, Marc Petit<sup>c</sup>, Bruno Bujoli<sup>c</sup>, Sylvain Bohic<sup>d</sup>, Pierre Weiss<sup>a,\*</sup>

<sup>a</sup>INSERM, UMRS 791, Université de Nantes, Laboratoire d'Ingénierie Ostéo-Articulaire et Dentaire, Faculté de chirurgie dentaire, 1 Place Alexis Ricordeau, 44042 Nantes Cedex 1, France

<sup>b</sup>Ecole Nationale vétérinaire de Nantes, Service de chirurgie expérimentale, Atlanpôle – La Chantrerie, BP40706, 44307 Nantes Cedex 3, France

<sup>c</sup>CNRS, UMR 6230, Université de Nantes, Chimie et Interdisciplinarité: Synthèse Analyse Modélisation, UFR Sciences et Techniques, 2 Rue de la Houssinière, BP92208, 44322 Nantes Cedex 03, France

<sup>d</sup>INSERM, U836, Equipe Rayonnement Synchrotron et Recherche Médicale, Grenoble Institut des Neurosciences, ESRF, 6 Rue Jules Horowitz, BP220, 38043 Grenoble Cedex 1, France

### ARTICLE INFO

#### Article history:

Received 10 September 2008

Accepted 27 November 2008

Available online xxx

#### Keywords:

Bone healing

Hydrogel

Degradation

*In vivo* test

Fluorescence

Siloxane

### ABSTRACT

In this paper we report a new method that permitted for the first time to selectively track a polysaccharide-based hydrogel on bone tissue explants, several weeks after its implantation. The hydrogel, which was developed for bone healing and tissue engineering, was labelled with a ruthenium complex and implanted into rabbit bone defects in order to investigate its *in vivo* degradation. 1, 2, 3 and 8 weeks after surgery, the bone explants were analyzed by synchrotron X-ray microfluorescence, infrared mapping spectroscopy, scanning electron microscopy, and optical microscopy after histological coloration. The results showed that the labelled polysaccharide-based hydrogel was likely to undergo phagocytosis that seemed to occur from the edge to the center of the implantation site up to at least the 8th week.

© 2008 Elsevier Ltd. All rights reserved.

### 1. Introduction

Nowadays, the needs for bone repair surgery focus more and more on sophisticated regenerative scaffolds, such as injectable calcium phosphate based material for minimally invasive surgical techniques [1–10]. In that context, two original devices made of biphasic calcium phosphate (BCP) granules suspended into polysaccharide-based media were designed in our laboratory about ten years ago [11–19]. The BCP granules are resorbable ceramic microspheres made of hydroxyapatite and  $\beta$ -tricalcium phosphate in a 60/40-weight ratio, respectively. The polysaccharide-based media are 3 wt% aqueous solutions of a hydroxypropylmethylcellulose (HPMC) or its silylated derivative (HPMC–Si) [20–22]. The latter can form a crosslinked hydrogel at physiological pH. In fact, the alkoxysilane groups present on this polysaccharide hydrolyze and condensate to form Si–O–Si (siloxane) bonds by varying the pH from basic to neutral. The resulting silylated Injectable Calcium Phosphate Ceramic Suspension (ICPCS–Si) self-sets into a hard 3D scaffold once injected into

bone defects, thus avoiding its dispersion around the implantation site.

In previous *in vitro* and *in vivo* investigations, the ICPCS–Si material showed a satisfying biocompatibility and bioactivity [23] making it worthwhile to be considered for clinical trials, in addition to the fact that the HPMC–Si hydrogel itself showed promising properties for tissue engineering [24–29]. For those purposes it is essential to understand the degradation of the ICPCS–Si material and particularly, the HPMC–Si hydrogel. It is well known that the BCP granules can solubilize into body fluids and be resorbed by osteoclasts [30], but no investigation was done about the degradation of the HPMC–Si polymer. This cellulose derivative could be degraded by cellulase into  $\beta$ -glucose units similarly to cellulose, but besides some plants and animals, such as micro-organisms and ruminants, most of the animals, including humans, do not produce this enzyme. Therefore, the polymer may diffuse into body fluids or may be degraded by phagocytes, unless it is not removed from the implantation site. To address this issue, it was necessary to track the polymer after its *in vivo* implantation. No histological coloration permitted to selectively do that as the bone tissue contains other types of carbohydrate-based compounds. The solution was then to label the polymer prior to implantation, and consequently to develop a labelling method that would be in accordance with the

\* Corresponding author. Tel.: +33 240 412 914; fax: +33 240 083 712.

E-mail address: [pweiss@sante.univ-nantes.fr](mailto:pweiss@sante.univ-nantes.fr) (P. Weiss).

conditions of use of the polymer, with long-term experiments, and with an analytical method of bone explants. Considering the limits of radiolabelling techniques, we proposed [31] to synthesize a ruthenium-based label that can be selectively detected by X-ray microfluorescence under synchrotron radiation, and that will be covalently bonded to the polymer *via* Si–O–Si bonds. Briefly, the label is a silylated tris-bipyridine ruthenium complex that is mixed with the HPMC–Si polymer in water at pH 12.4. After addition of an acid buffer, the silanolate groups present on both compounds randomly cross-condensate into Si–O–Si bonds to form a labelled hydrogel at pH 7.4 (Fig. 1).

In the present paper, this labelling method was used to probe the HPMC–Si and ICPCS–Si materials after their implantation into femoral epiphysis defects of rabbits. 1, 2, 3 and 8 weeks after surgery, the animals were sacrificed and the resulting explants were analyzed by synchrotron X-ray microfluorescence, infrared mapping microscopy, scanning electron microscopy, and also by optical microscopy after Movat colorations. Prior to the main study, the cytotoxicity of the labelled materials was evaluated by *in vitro* and *in vivo* assays.

## 2. Materials and methods

### 2.1. Preparation of the ruthenium labelled HPMC–Si hydrogel and ICPCS–Si

All the following procedures were performed under sterile conditions. 7.5 mg (6.5  $\mu\text{mol}$ ) of bis(2,2'-bipyridine)(5-methyl-5'-(3-(triethoxysilyl)propylcarbamoyloxy)methyl-2,2'-bipyridine)ruthenium (II) bis(hexafluorophosphate) prepared as previously described [31] were mixed with 8 ml of a steam sterilized 3 wt% basic aqueous solution (pH = 12.4) of a silylated hydroxypropylmethylcellulose (HPMC–Si) [20]. Briefly, the HPMC–Si polymer is a commercial hydroxypropylmethylcellulose (E4 M<sup>®</sup>, Colorcon-Dow chemical, France) modified by 3-glycidoxypropyltrimethoxysilane *via* a nucleophilic epoxide opening that occurred under heterogeneous conditions. The resulting Si content of the polymer used herein was  $0.59 \pm 0.03$  wt%.

Case 1 (unrinsed and *in situ* crosslinked materials): similarly to the typical conditions of use of the HPMC–Si and ICPCS–Si materials [12], 1 volume of 4-(2-hydroxyethyl)piperazine-1-ethanesulfonic acid (HEPES) buffer A (pH = 3.6) or 0.5 volume of HEPES buffer B (pH = 3.2) was mixed with 1 volume of the basic mixture of HPMC–Si/ruthenium complex, and in case of labelled ICPCS–Si implantations, 40 or 50 wt% of BCP granules of either 40–80  $\mu\text{m}$  (from Biomatlante, France) or 80–200  $\mu\text{m}$  [32,33] were also added, respectively. One hour to one hour and a half after the addition of the buffer, and while the viscosity of the mixture was low enough (about 0.05–0.2 Pa.s without the BCP granules) [34], 0.5 ml of labelled HPMC–Si or

ICPCS–Si were implanted per rabbit bone defect. In case 1, the labelling reaction was not allowed for completion, which implied that a part of the unattached label may have diffused around the implantation sites.

Case 2 (rinsed and *ex situ* crosslinked materials): as a control of the possible label dispersion, the typical conditions of use of the HPMC–Si hydrogel and ICPCS–Si were modified. The labelling procedure was thus carried out in culture wells and the resulting mixtures were left up to 14 days in order to optimize the yield of the labelling reaction (previous visco-elastic measurements of the hydrogel during its reticulation showed 80% of reaction progression after 48 h and 100% after 3 weeks). Each sample was then rinsed several times with deionized water until colorless solutions were obtained (the label is orange). According to previous labelling studies, the percentage of label covalently linked to the polymer reach about 30% of the initial loading (i.e. 830 ppm of Ru) [31]. Fragments of the resulting self-hardened labelled hydrogel and ICPCS–Si were then introduced into rabbits bone defects and also into subcutaneous pockets in case of labelled hydrogels only (see below §2.3). Contrary to case 1, the materials were reticulated and washed to remove unattached label prior to implantation.

### 2.2. Viability of chondrocytes cultured in presence of labelled HPMC–Si hydrogel

The human chondrocytic cell line SW1353 [35] was cultured in DMEM/Ham's F-12 medium supplemented with 10% FCS, 1% penicillin/streptomycin and 1% L-glutamine (culture medium) and incubated at 37 °C in a humidified atmosphere of 5% CO<sub>2</sub>. Culture medium was changed every 2–3 days. Cellular viability was measured using a Methyl Tetrazolium Salt (MTS) assay as previously described [36,37]. Briefly, SW1353 were allowed to attach in 24-well plates at a final density of 10,000 cells/cm<sup>2</sup>. After 24 h, culture medium was removed and 500  $\mu\text{l}$  of rinsed ruthenium labelled hydrogel (case 2) were added in each well. Samples were incubated at 37 °C for 4 h before adding 1 ml of culture medium. As controls, cells were also cultured in absence of labelled hydrogel (control A), and in presence of actinomycin-D (5  $\mu\text{g}/\text{ml}$ ), an inhibitor of RNA polymerase [38], which was used as a potent inducer of cell death. After 1, 2 and 7 days, hydrogel and culture media were removed and a MTS solution was added in each well for 1–3 h according to the manufacturer's instructions. Finally, colorimetric measurements of formazan dye were performed on a spectrophotometer with an optical density reading at 490 nm. Results were expressed as relative MTS activities compared to the control A. Each experiment was repeated at least twice with similar results. Results are expressed as mean  $\pm$  SEM of triplicate determinations. Comparative studies of means were performed by using one-way ANOVA followed by post hoc test (Fisher's projected least significant difference) with a statistical significance at  $P < 0.001$ .

### 2.3. Animal model and surgical procedures

All animal handling and surgical procedures were conducted according to European Community guidelines for the care and use of laboratory animals (DE 86/609/CEE). The study was approved by the local animal care and safety committee. The experiments were performed according to Good Laboratory Practices (GLP) at the Veterinary School of Nantes.

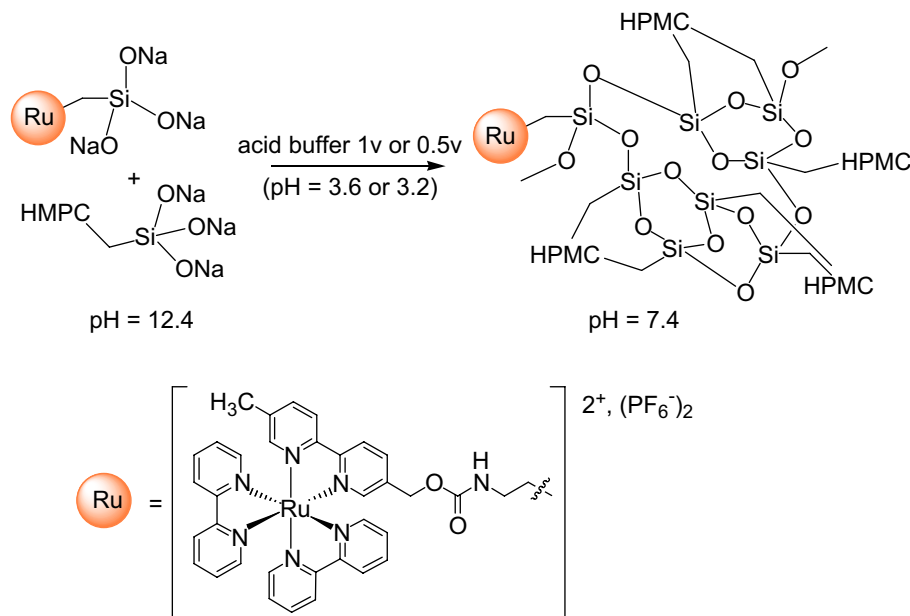
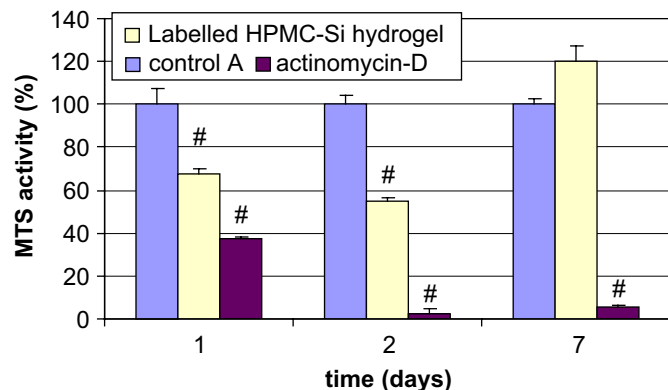


Fig. 1. Labelling method of the HPMC–Si polymer.



**Fig. 2.** Cellular viability of SW1353 chondrocytes cultured in the absence (control A) or in the presence of rinsed labelled HPMC-Si hydrogel (case 2), or in the presence of actinomycin-D (5  $\mu\text{g}/\text{ml}$ ) over 1, 2 and 7 days. MTS activities are expressed as relative MTS activities compared to the control A (#:  $P < 0.001$ ).

Eleven adult female New Zealand White (NZW) rabbits weighing approximately 3–4 kg were purchased from a professional breeder (Charles River Laboratories, L'Arbresle, France). The animals were placed in quarantine for at least 10 days prior to surgery. General anesthesia was performed using an intramuscular injection of ketamine (Imalgène 1000<sup>®</sup>, Merial, Lyon, France) and xylazine (Rompun<sup>®</sup>, Laboratoire Bayer Pharma, Puteaux, France). The anesthesia was maintained by intravenous injection with a mixture of ketamine and xylazine.

#### 2.3.1. Subcutaneous implantation

The lumbar area was shaved, disinfected and prepared for surgery. The skin was incised, small pockets were created with blunt dissection, then filled with ruthenium labelled or unlabelled HPMC-Si hydrogels (2 independent sites per animal). Skin was sutured using degradable sutures (Polysorb<sup>®</sup> 3-0, France).

#### 2.3.2. Femoral implantation

The animals were surgically prepared by shaving both limbs, skin disinfection with iodine solution and sterile draping. A longitudinal skin incision was made to expose the distal lateral femoral condyle. A critical defect [39] of 6 mm in diameter and 10 mm in depth was created at the epiphyseal-metaphyseal junction by using a motor-driven drill (Aesculap, Tuttlingen, Germany). The drilling process was achieved in 3 successive steps using burs of 2, 4, and 6 mm in diameter. During the drilling process, the defect site was continuously irrigated using a syringe of sterile saline solution. Bone chips and particles were removed from the defects by irrigation with saline solution. The defects were then packed with sterile swabs gauzes until bleeding had subsided. The femoral cavity was then filled with either ruthenium labelled or unlabelled materials (HPMC-Si hydrogel or ICPCS-Si). The subcutaneous tissues and skin were closed in different layers using degradable sutures (Safil déc.3<sup>®</sup> B. Braun Laboratory, France). The surgical site was finally covered with an adhesive bandage.

No prophylactic antibacterial or anti-inflammatory treatments were administered after surgery. 1, 2, 3 and 8 weeks after implantation, the animals were anaesthetized and sacrificed by intracardiac overdose of sodium pentobarbital.

#### 2.4. Preparation of thin bone sections

Some of the rabbit bone explants (issued from case 1) were fresh-frozen cut into 30–150  $\mu\text{m}$ -thick slices at  $-20^\circ\text{C}$  with a Jung CM3000 cryomicrotome (Leica, France) equipped with a steel blade. The explants were previously fixed on the removal sample stand of the apparatus with Tissue-Tek<sup>®</sup> O.C.T. (Optimal Cutting Temperature) compound (from Miles, diagnostics division, USA) by immersion into liquid nitrogen. Once the fresh-cutting was achieved, those bone explants, as well as the other ones (issued from case 2), were dehydrated by successive immersions into baths of 10% formol, and ethanol/acetone of gradient concentrations prior to being embedded into glycolmethylmethacrylate (GMMA). The resulting resin blocks were cut into 7–200  $\mu\text{m}$ -thick slices on a Leica SM2500 (France) equipped with a tungsten blade.

#### 2.5. Synchrotron X-ray microfluorescence analysis

Synchrotron X-ray microfluorescence analysis was performed on fresh-frozen and resin embedded bone slices on the beamline ID18F (6–28 keV,  $1.5 \times 12 \mu\text{m}^2$ ) at ESRF (Grenoble, France) and on the beamline L (2–80 keV,  $30 \times 30 \mu\text{m}^2$ ) at Hasylab (Hamburg, Germany). The ruthenium, calcium, and iron K alpha emission bands (noted RuK $\alpha$ , CaK $\alpha$ , and FeK $\alpha$ ) were measured at 19.15 keV, 3.69 keV, and 6.39 keV, respectively. The fitting and the plotting of the data were obtained using the PyMca software.

#### 2.6. Histological and histomorphometrical analysis

Only the resin embedded bone slices of 7  $\mu\text{m}$ -thick were stained with Movat's pentachrome [40,41] and then analyzed on a Nikon Eclipse TE2000-E Inverted Microscope (Solent Scientific limited, France). Some resin embedded bone blocks were coated by a gold/palladium alloy prior to being analyzed by Scan Electronical Microscopy on a LEO 1450 VP. The image processing was run on a Leica Quantimeter 500 (Cambridge, UK).

#### 2.7. FTIR analysis

Before FTIR analysis, the sections were polished using silicon carbide paper and a variable speed grinder-polishing machine (Buehler, model Metaserv 2000). The micro-infrared spectra were recorded on a Magna IR 550 spectrometer (Nicolet) coupled to a ThermoElectron Continuum microscope ( $\times 15$  ThermoElectron Infinity corrected Refflachromat objective), with a mercury-cadmium-telluride detector (MCT-A). The transmission spectra were carried out on thin sections (7  $\mu\text{m}$ ) deposited on a BaF<sub>2</sub> window. The data were acquired with a spatial aperture size of  $25 \times 25 \mu\text{m}^2$ , in the range of  $4000\text{--}750 \text{ cm}^{-1}$  at  $4 \text{ cm}^{-1}$  resolution. Typical step size was 25  $\mu\text{m}$ . The Attenuated Total Reflectance (ATR) measurements were recorded with a micro slide-on ATR germanium cone-shaped tip crystal (single reflection, medium incidence angle  $\approx 25^\circ$ , refractive index = 4). The ATR accessory was fixed directly on the  $\times 15$  objective. The aperture size was adjusted to  $50 \times 50 \mu\text{m}^2$  resulting in investigated areas of about  $12.5 \mu\text{m} \times 12.5 \mu\text{m}$ . The spectral range was  $4000\text{--}650 \text{ cm}^{-1}$  at  $4 \text{ cm}^{-1}$  resolution. Step size was fixed at 20  $\mu\text{m}$ . All the spectra were corrected from residual H<sub>2</sub>O and CO<sub>2</sub> absorptions and automatically smoothed and baseline treated, using OMNIC software (ThermoFisherScientific). In each case, GMMA peaks were subtracted. Different chemigram profile setups were chosen for

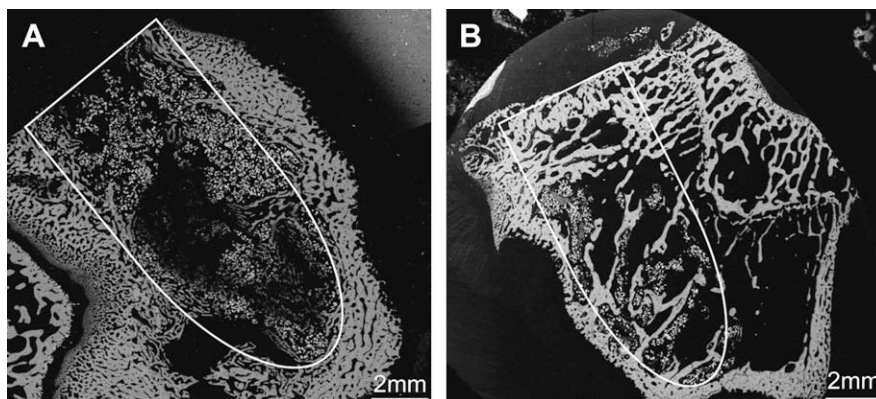


**Fig. 3.** SEM images showing new bone formation within femoral epiphysis defects of rabbits filled with rinsed labelled ICPCS-Si (case 2) over 2 weeks (A) and 8 weeks (B). (Magnification  $\times 5$ ).

the corresponding expected components. The resulting profiles were obtained by integrating the area under the peaks at  $1700\text{--}1600\text{ cm}^{-1}$  (amide I) and  $1200\text{--}900\text{ cm}^{-1}$  ( $\nu_1, \nu_3$  phosphate).

### 3. Results

#### 3.1. Viability of chondrocytes cultured in the presence of the labelled HPMC–Si hydrogel

The viability of SW1353 chondrocytes cultured in 2D in the presence of the rinsed labelled hydrogel was examined by MTS assays realized after 1, 2 and 7 days. The results (Fig. 2) showed that for 1 and 2 days of culture, the presence of the labelled hydrogel reduced the MTS activity of chondrocytes by 30 and 45%, respectively. During the first 2 days, an undefined portion of the culture media is absorbed by the hydrogel, making the nutrients probably less available for the cells. However, after 7 days and several renewals of culture media, there was no significant variation of the MTS activity between the chondrocytes cultured in the presence and in the absence of the labelled hydrogel. The cells seemed to have recovered their activity, probably because of an increase of the culture media availability due to the saturation of the hydrogel. The labelled hydrogels seemed to be non-cytotoxic after 1 week of cell culture.

#### 3.2. Evaluation of the *in vivo* biocompatibility of the labelled HPMC–Si hydrogel and ICPCS–Si

In subcutaneous and bone implantation sites, no evidence of adverse foreign body reaction was observed in the presence of the rinsed labelled materials as compared to the controls (unlabelled materials). The subcutaneous explants showed that both labelled and unlabelled hydrogels were encapsulated into a fibrous tissue whose edge was invaded by macrophagic cells. No vascular or cellular invasion occurred within these implants, but the amount of hydrogel was significantly lower after 8 weeks as compared to 2 weeks. In contrary, the bone explants showed the presence of vessels and cells within the implants but no evidence of osteolysis or formation of fibrous interface for both labelled and unlabelled ICPCS–Si. After inclusion into resin, these bone explants were analyzed by scanning electron microscopy to compare the osseointegration of the labelled and unlabelled materials [23]. Considering the number of rabbits implied in this study (3 per condition), only qualitative comparisons were made, showing no remarkable difference between the both materials. After 2 weeks (Fig. 3A) trabecular bone ingrowths were present at the periphery of the bone defect mainly, whereas after 8 weeks (Fig. 3B) the bone colonization has significantly increased and extended to the center of the implant.

#### 3.3. Distribution of ruthenium labelled HPMC–Si hydrogels within the implantation sites after 1, 2, 3 and 8 weeks

##### 3.3.1. Unrinsed and *in situ* crosslinked labelled hydrogels (case 1)

1 and 3 weeks after implantation in femoral epiphysis defects of rabbits, the X-ray microfluorescence analysis performed on fresh-frozen slices from the explants showed that most of the ruthenium was dispersed all over the bone area surrounding the implantation site (Fig. 4a–c). Inside the defect itself, very low proportions of ruthenium were observed, as well as an accumulation of iron, which may result from the bleeding during the surgical operation. After inclusion into GMMA resin, the same explants were thin cut ( $7\ \mu\text{m}$ ), and the resulting deeper sections were stained by a Movat coloration prior to being observed by optical microscopy. The images (not shown) revealed that the implantation sites were filled with some dehydrated hydrogel surrounded by a connective tissue

and some unidentified cells. The dehydration of the hydrogel and the difficulties in identifying the cells were a consequence of the frozen cutting.

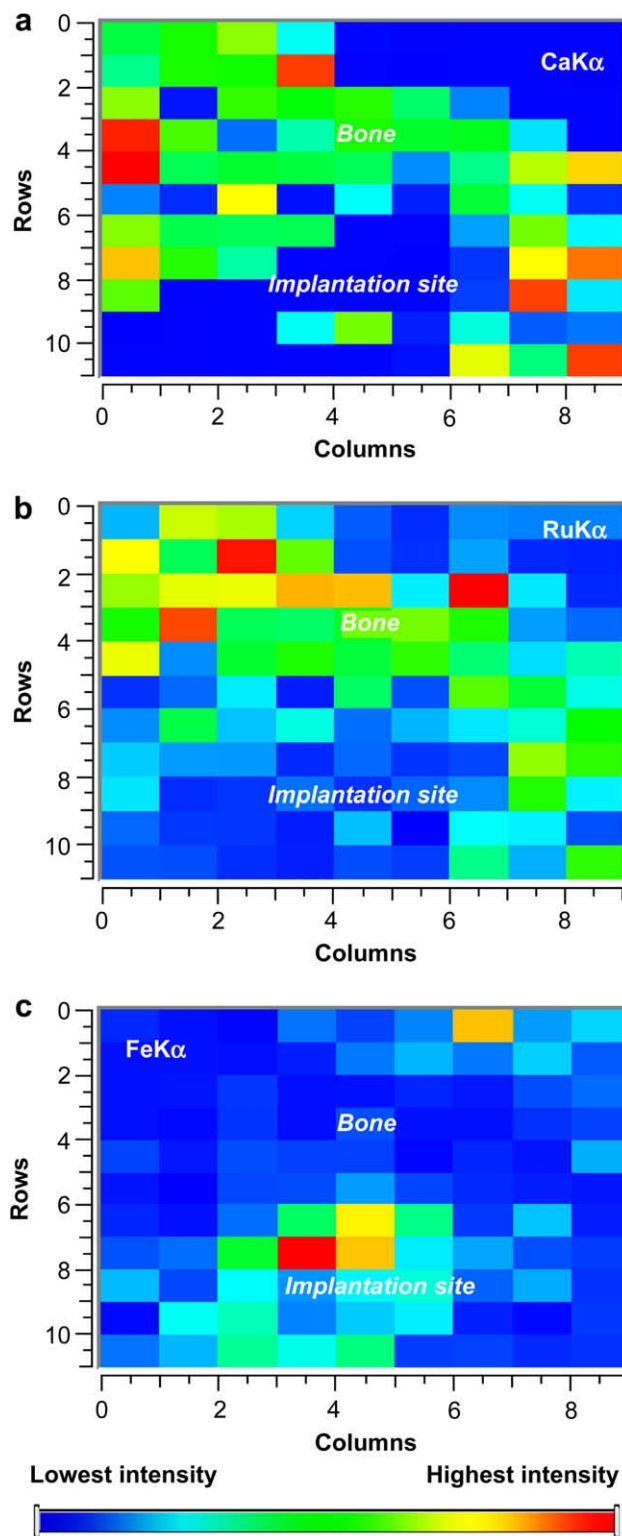


Fig. 4. Unrinsed and *in situ* crosslinked labelled HPMC–Si hydrogel (case 1) 3 weeks after implantation in the femoral epiphysis defect of a rabbit. X-ray microfluorescence analysis of a  $150\text{-}\mu\text{m}$ -thick fresh-frozen slice from the explant: CaK $\alpha$  (a), RuK $\alpha$  (b) and FeK $\alpha$  (c) (maps of  $5000 \times 5000\ \mu\text{m}^2$ , steps of  $625 \times 500\ \mu\text{m}^2$ , 80 s of acquisition per pixel, beamline 6–28 keV  $1.5 \times 12\ \mu\text{m}^2$ ).

### 3.3.2. Rinsed and ex situ crosslinked labelled hydrogels (case 2)

After 2 weeks, the ruthenium was mainly located inside the bone defect and trabeculae (Fig. 5a). No dispersion of ruthenium all over calcium areas was found. The micro-infrared analysis using an Attenuated Total Reflectance (ATR) method allowed localizing mineralized bone areas via the phosphate vibration bands  $\nu_1$  and  $\nu_3$  at 1200–900  $\text{cm}^{-1}$ , and the protein areas via the amide I vibration band at 1700–1600  $\text{cm}^{-1}$ . The spectra acquired along a virtual line of 2.2 cm crossing a bone stripe and two separated ruthenium areas (Fig. 5b) confirmed the presence of phosphate and proteins in the bone stripe. It also showed the penetration of proteins inside the labelled hydrogel area up to 0.2 cm in depth from the edge of the mineralized bone zone. A Movat coloration of the same bone section revealed the presence of polynucleated macrophages and vessels within the implantation site, around the rest of the hydrogel (Fig. 5c). After 8 weeks, only very few areas of low ruthenium concentration were still present. In fact, only 1 of 3 explants showed a detectable amount of ruthenium, which was accumulated in a well-defined area

inside the bone defect (Fig. 6), and surrounded by macrophages (not shown).

### 3.4. Distribution of ruthenium labelled ICPCS–Si within the implantation site after 1, 2, 3 and 8 weeks

The X-ray microfluorescence analysis of the *ex situ* crosslinked labelled ICPCS–Si material before implantation showed that the ruthenium label tended to concentrate around calcium phosphate granules (Fig. 7). Observations were similar with implanted materials (see below).

#### 3.4.1. Unrinsed and in situ crosslinked labelled ICPCS–Si (case 1)

After 1 week, the ruthenium was located near the calcium phosphate granules, which means from the center of the defect up to its edge (Fig. 8a). A moderate diffusion of the ruthenium over the mineralized bone area was observed only at the periphery of the implantation site, where the osseo-integration of the calcium phosphate granules first took place as seen after a Movat coloration

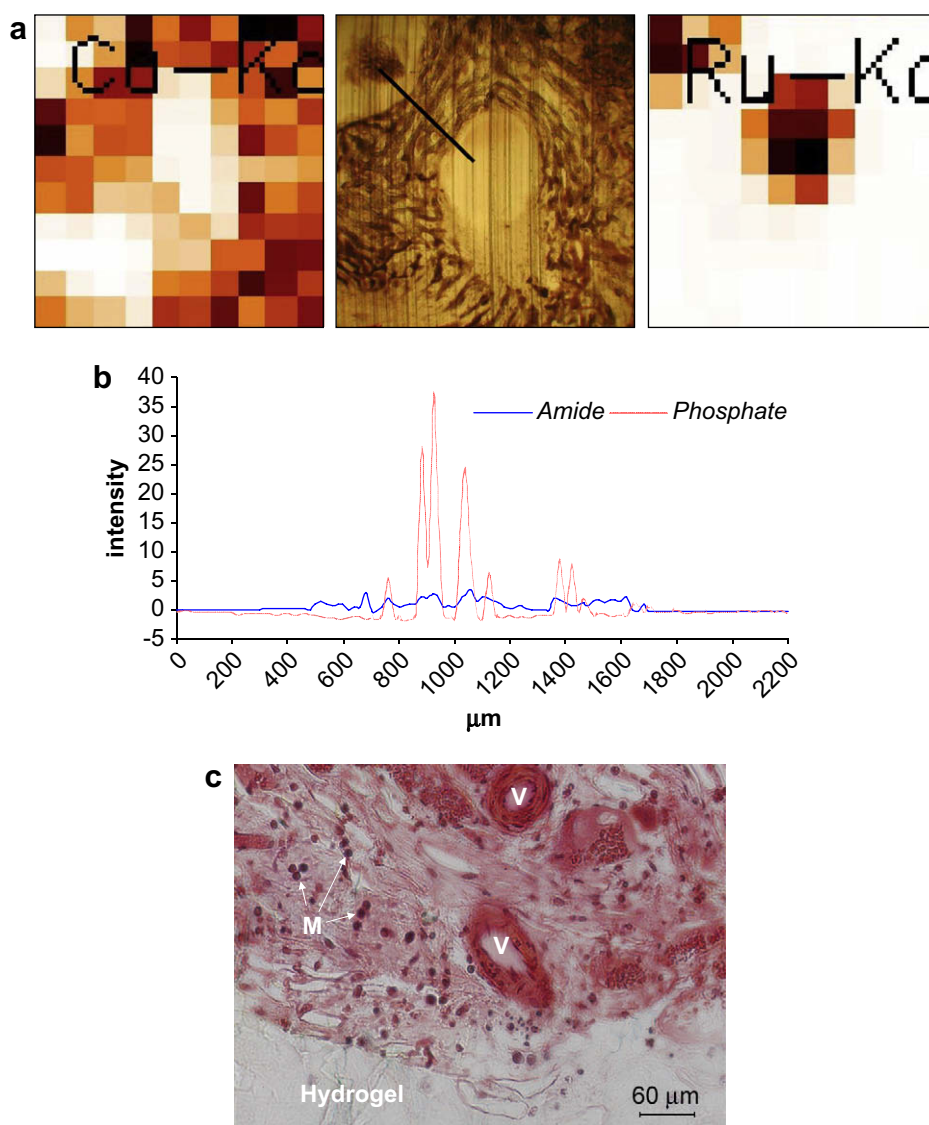


**Fig. 5.** Rinsed and *ex situ* crosslinked labelled HPMC–Si hydrogel (case 2) 2 weeks after implantation in the femoral epiphysis defect of a rabbit. (a) X-ray microfluorescence analysis of a 200- $\mu\text{m}$ -thick resin embedded slice from the explant: CaK $\alpha$  (left), scanned area (middle) and RuK $\alpha$  (right) (maps of 2538  $\times$  3450  $\mu\text{m}^2$ , steps of 350  $\times$  350  $\mu\text{m}^2$ , acquisition time of 150 s per pixel, beamline 2–80 keV 30  $\times$  30  $\mu\text{m}^2$ ). (b) Infrared scanning by ATR within the implantation site (line (in black above) of 2.2 mm, steps of 20  $\mu\text{m}$ , 30 scans per pixel). (c) Optical microscope image after a Movat coloration (V = vessel, M = macrophage).

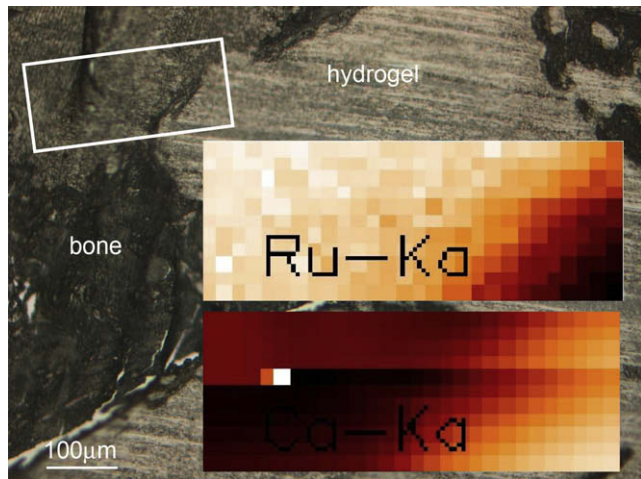


**Fig. 6.** Rinsed and *ex situ* crosslinked labelled HPMC–Si hydrogel (case 2) 8 weeks after implantation in the femoral epiphysis defect of a rabbit. X-ray microfluorescence analysis of a 90- $\mu\text{m}$ -thick resin embedded slice from the explant: RuK $\alpha$  (upper) and CaK $\alpha$  (lower) (maps of  $279 \times 100 \mu\text{m}^2$ , steps of  $10 \times 10 \mu\text{m}^2$ , acquisition time of 100 s per pixel, beamline 2–80 keV  $30 \times 30 \mu\text{m}^2$ ).

of the explant (Fig. 8b). The optical microscope image clearly showed that the calcium phosphate granules (blue) were surrounded and interconnected by osteoids (red). After 3 weeks, the distribution of the ruthenium probe was similar, and the implanted material was surrounded by polynucleated macrophages (not shown).

#### 3.4.2. Rinsed and *ex situ* crosslinked labelled ICPCS–Si (case 2)

After 2 weeks, the distribution of the ruthenium seemed to be less homogeneous over the calcium phosphate granules, and did not expand to the peripheral mineralized bone areas (Fig. 9a–b). Additional infrared analysis (Fig. 9c) showed the presence of proteins over the surrounding mineralized bone areas as well as within the implantation site where no calcium phosphate was present. The histological analysis of the same sample revealed the presence of macrophages within the defect (not shown). After 8 weeks, only few ruthenium areas were detectable, which were systematically located near calcium phosphate granules (Fig. 10a). Once again, many macrophagic cells were observable around the ICPCS–Si material (Fig. 10b, right). Further infrared analysis also

showed the presence of proteins inside and near new mineralized bone areas located at the periphery of the implanted material (Fig. 10c).

## 4. Discussion

The probing method used in this work is a new technique that permitted for the first time to selectively localize a polysaccharide-based hydrogel on bone tissue explants after several weeks of implantation. In the same fashion it would be possible to track various type of compounds by modulating the grafting group of the ruthenium label (i.e. the alkoxy silane group). It may be an efficient alternative to radionuclid labelling techniques, which imply expensive specific equipment and short-term experiments (only few days). Synchrotron X-ray microfluorescence is an interesting analytic method to map tissue slices. The main limit of this technique is the acquisition time, which depends on the concentration of the tracked element, the size and the thickness of the sample, the number of recorded pixels, and the size of the beamline (e.g. HASYLAB and ERSF beamlines are different). For example, to map a  $100 \times 100\text{-}\mu\text{m}^2$  area with a high resolution (steps not greater than the size of the beamline) and an acquisition time of 100 s per pixel would take about 17 h at the ESRF. Thus, low-resolution mapping and line scans were the quickest way to analyze few millimetre square areas, in addition to the fact that the access to the beamlines was limited. The combination of X-ray microfluorescence with more classical analytical methods, such as infrared mapping, SEM, and histological coloration, led to the needed information.

Firstly, we showed no evidence of cytotoxicity due to the presence of the ruthenium label on HPMC–Si hydrogels after 7 days of cell culture. The osseo-integration of the ICPCS–Si materials seemed to qualitatively remain the same in the presence or in the absence of the label. Those results confirmed the relevance of our labelling method. The use of chondrocytes cells, which are specific to cartilage applications, referred to a previous cytotoxicity assays realized in the presence of the unlabelled HPMC–Si hydrogel for a study concerning the use of the HPMC–Si hydrogels in cartilage tissue engineering [42]. We presumed that the results would likely be similar with MC3T3 cells, which are specific to bone applications.

A limited number of rabbits (11) were implanted in order to minimize the number of sacrificed animals and to reduce the time and the cost of the present study. Various implantation times were

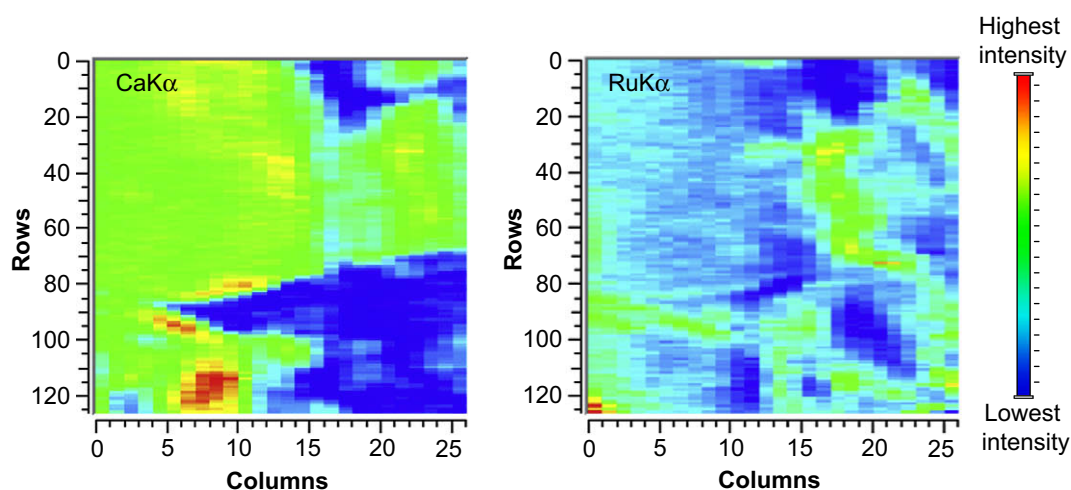


**Fig. 7.** *Ex situ* crosslinked labelled ICPCS–Si before implantation. X-ray microfluorescence mapping of a 60- $\mu\text{m}$ -thick fresh-frozen slice (map of  $250 \times 250 \mu\text{m}^2$ , steps of  $10 \times 12 \mu\text{m}^2$ , acquisition time of 5 s per scan, beamline 6–28 keV  $1.5 \times 12 \mu\text{m}^2$ ).

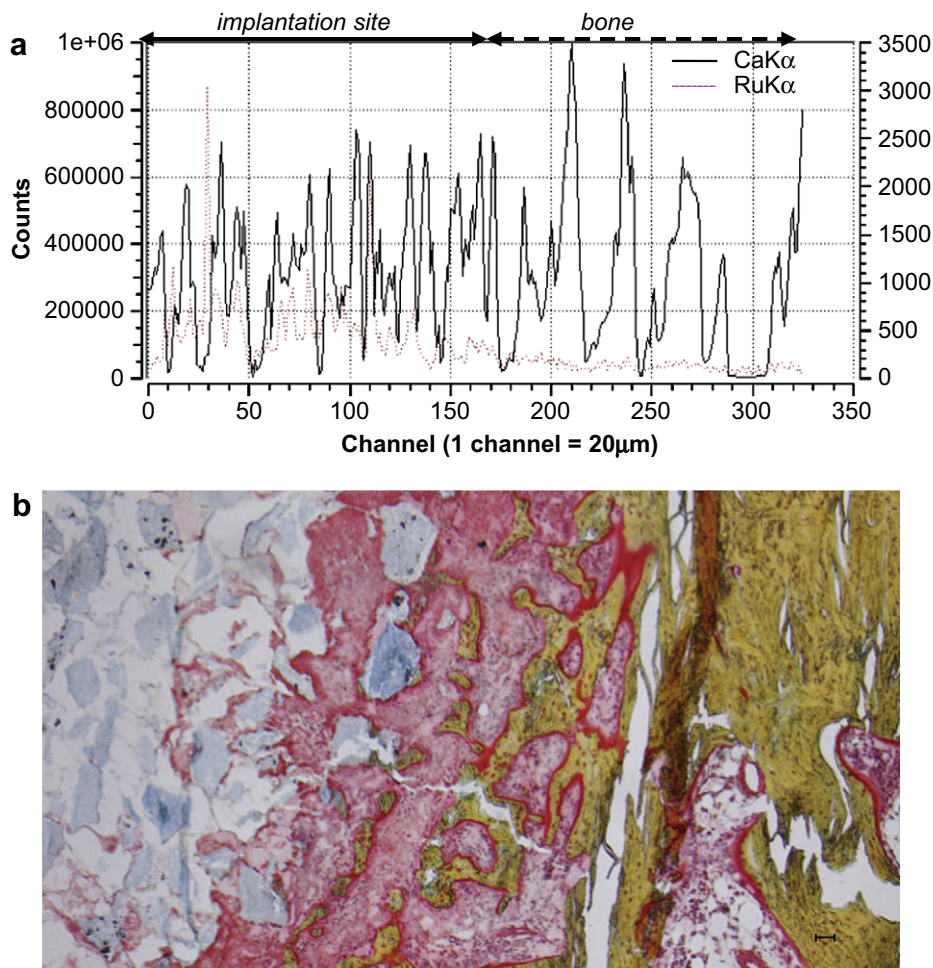


**Fig. 8.** Unrinsed and *in situ* crosslinked labelled ICPCS–Si (case 1) 1 week after implantation in the femoral epiphysis defect of a rabbit. (a) X-ray microfluorescence analysis of a 30  $\mu\text{m}$ -thick fresh-frozen slice from the explant (line of 6500  $\mu\text{m}$ , steps of 20  $\mu\text{m}$ , acquisition time of 100 s per pixel, beamline 6–28 keV  $1.5 \times 12 \mu\text{m}^2$ ). (b) Optical microscope image after a Movat coloration (magnitude  $\times 10$ ).

chosen: 2 and 8 weeks for the *ex situ* crosslinked materials (case 2) in comparison with typical protocols found in the literature, and shorter times (1 and 3 weeks) for the *in situ* crosslinked materials (case 1), as the ruthenium label was likely to disperse prior to binding to the polysaccharide. Also, considering the unattached ruthenium label, we chose to fresh-frozen cut the bone explants issued from case 1 for the X-ray microfluorescence analysis as the ethanol/acetone bathing step of the resin embedding protocol may have removed the unattached ruthenium label off the samples.

Case 1 (unrinsed and *in situ* crosslinked materials) was supposed to reflect the typical way of use of the ICPCS–Si material in bone healing applications. The limit of the labelling reaction (slow and incomplete) led to case 2 (rinsed and *ex situ* crosslinked materials), which in a certain way reflects the use of the HPMC–Si in tissue engineering applications (i.e. implantation of a reticulated hydrogel with embedded cells) [28,42]. Also, considering that the materials are normally injected slightly before their gelation time, we expected that the degradation profile of the *ex situ* crosslinked materials would be similar to the *in situ* ones, at least on a long-term basis, such as 2 weeks or more.

As expected for the unrinsed and *in situ* crosslinked materials (case 1), the results showed that the ruthenium probe had not enough time to react with the polymer prior to being in contact with the animal body fluids, which resulted in a dispersion of the unattached label around the implantation sites. This was particularly relevant for the hydrogel 3 weeks after implantation, for

which the ruthenium has spread all over the surrounding mineralized bone.

For the rinsed and *ex situ* crosslinked materials (case 2), the ruthenium probe was detected within the implantation sites only, which indicated that the label was properly attached to the polymer. Thus, the distribution of the ruthenium better reflected the location of the probed materials. The results showed that the HPMC–Si hydrogel did not diffuse within the bone matrix and that it was detectable after at least 8 weeks in the limits of our experimental conditions (the probe loading, the amount of implanted hydrogel, the thickness of the bone slices, and the characteristics of the synchrotron beamlines). After 8 weeks, only few areas of low ruthenium concentration were found as compared to 2 weeks of implantation. Those areas were systematically located inside the implantation sites, near BCP granules or new bone ingrowths when present. This demonstrated that the HPMC–Si hydrogel was mostly degraded or removed after 8 weeks, and that these phenomena were concomitant with the resorption of the BCP granules when present. Considering the macrophagic cells concentration around the remaining implanted materials and the significant decrease of the amount of hydrogel between 2 and 8 weeks, it seems reasonable to assume that the reticulated hydrogels underwent phagocytosis until at least the 8th week. This hypothesis would be in agreement with the observations of the subcutaneous implantations (see the biocompatibility assays), and a previous work reporting inflammatory reactions due to reticulated gels [43]. As seen on infrared maps

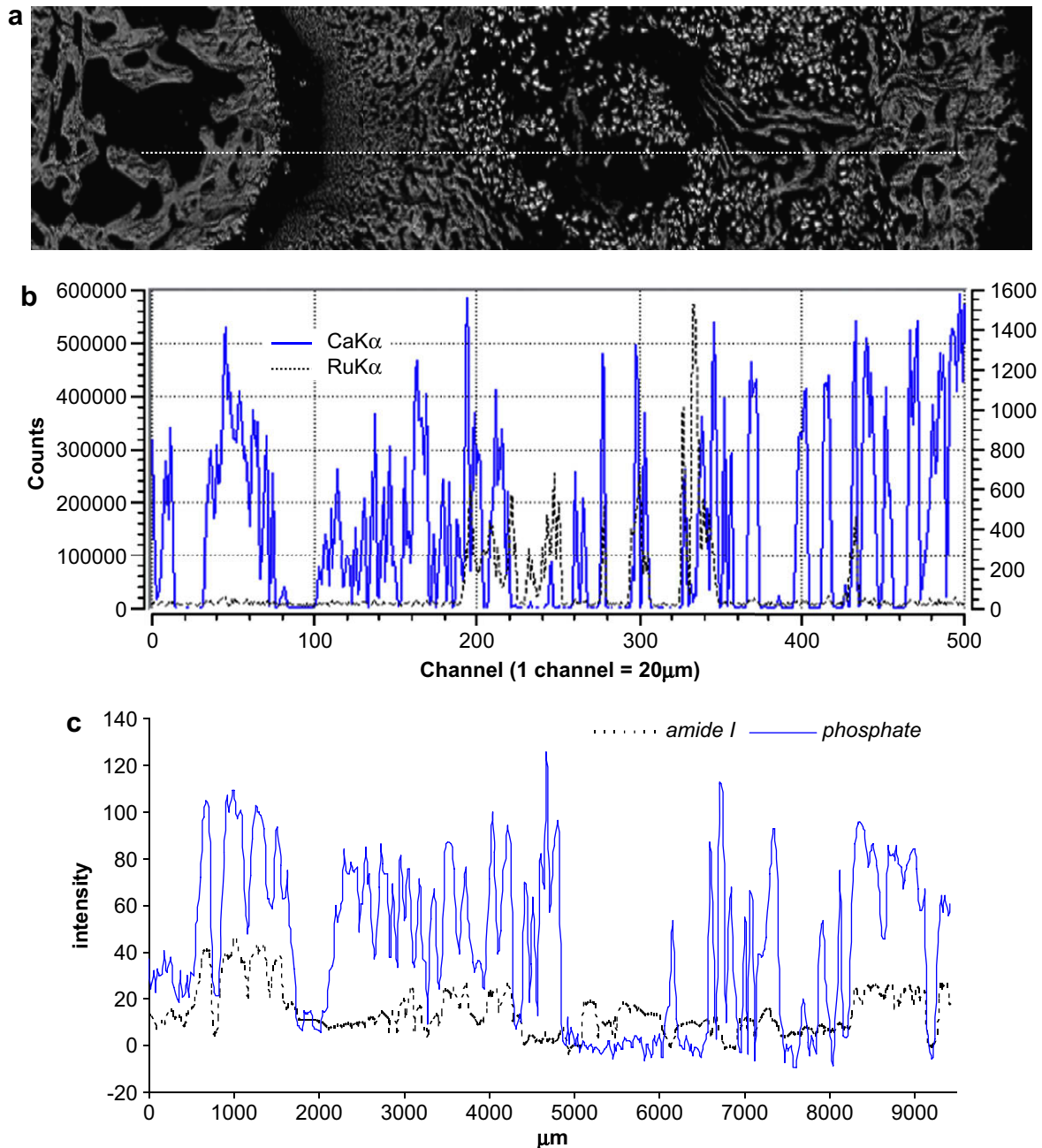


**Fig. 9.** Rinsed and *ex situ* crosslinked labelled ICPCS–Si (case 2) 2 weeks after implantation in the femoral epiphysis defect of a rabbit. Analysis of a 15- $\mu\text{m}$ -thick resin embedded slice from the explant: (a) SEM image of the analyzed area (white dotted line), (b) X-ray microfluorescence scans (line of 10,000  $\mu\text{m}$ , steps of 20  $\mu\text{m}$ , acquisition time of 120 s per pixel, beamline 6–28 keV  $1.5 \times 12 \mu\text{m}^2$ ), and (c) Infrared mapping by ATR (line of 9424  $\mu\text{m}$ , steps of 25  $\mu\text{m}$ , 30 scans per pixel).

after 2 weeks, the diffusion of proteins within the reticulated hydrogel seemed to be slow, probably because of the density of the network. However, after 8 weeks and in presence of BCP granules, some proteins were found within the implantation site, near new bone areas only. The resorption of the granules may then enhance the diffusion of protein within the materials.

## 5. Conclusion

The probing method used in this study permitted for the first time to well-localize a polysaccharide-based hydrogel several weeks after its implantation in bone defects in rabbits. This investigation allowed us to better understand the *in vivo* degradation of our HPMC–Si hydrogel, which is used in bone healing and

tissue engineering. As predicted, the results showed that the HPMC–Si hydrogel was likely to undergo phagocytosis that seems to occur from the edge of the implantation site to its center up to at least the 8th week. This demonstrated that the HPMC–Si hydrogel is biodegradable. Further investigations using X-ray fluorescence techniques at the nanoscale will be run to detect the presence of the hydrogel within the inflammatory cells and to confirm the suggested phagocytosis. The use of our ruthenium label or some analogues, along with the X-ray microfluorescence as a probe detection method might be extended to other *in vivo* biological evaluations. Indeed, the ruthenium probe seemed non-cytotoxic if well-attached to the substrate. It is absent from biological systems, and it can be selectively detected by X-ray microfluorescence even at low concentration (i.e. 0.5 ppm).

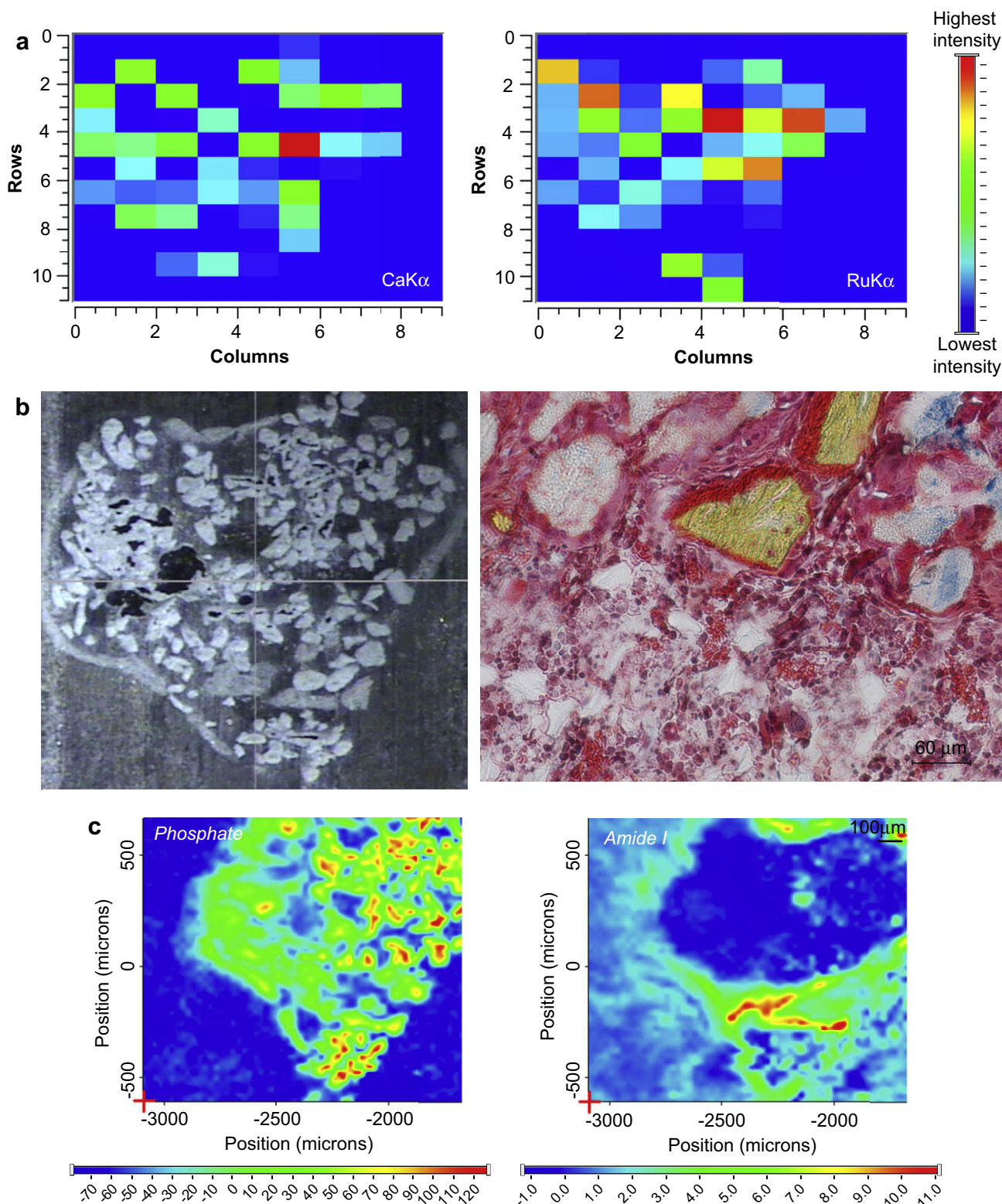


**Fig. 10.** Rinsed and *ex situ* crosslinked labelled ICPCS-Si (case 2) 8 weeks after implantation in the femoral epiphysis defect of a rabbit. (a) X-ray microfluorescence analysis of a 7  $\mu\text{m}$ -thick resin embedded slice from the explant (maps of  $1400 \times 1300 \mu\text{m}^2$ , steps of  $175 \times 130 \mu\text{m}^2$ , acquisition time of 100 s per pixel, beamline 6–28 keV  $1.5 \times 12 \mu\text{m}^2$ ). (b) Optical microscope images before (left, scanned area) and after a Movat coloration (right, zoom area, magnitude  $\times 20$ ). (c) Infrared mapping by transmission light on a 7- $\mu\text{m}$ -thick resin embedded slice from the explant (maps of  $1400 \times 1300 \mu\text{m}^2$ , steps  $25 \times 25 \mu\text{m}$ , 30 scans per pixel).

### Acknowledgements

We acknowledge financial support from the INSERM and the Région Pays de la Loire through CPER Biomatériaux S3 and Bioregos

grants, and PhD studentship (Samia Laïb). We also acknowledge the European Synchrotron Radiation Facility, DESY and the European Community for provision of synchrotron radiation facilities, and we would like to thank Sylvain Bohic and Karen Rickers for their

assistance in using beamlines ID18F and L, respectively. We also thanks Anne Moreau (Anapathologist at the Nantes Hospital) for her help in interpreting histological slices, Sophie Sourice for the histological colorations, Paul Pilet for the SEM images, and Biomatlante (Vigneux de Bretagne, France) for kindly giving MBCP® granules.

## Appendix

Figures with essential colour discrimination. Certain parts of the majority of figures in this article are difficult to interpret in black and white. The full colour images can be found in the on-line version, at doi:10.1016/j.biomaterials.2008.11.031.

## References

- Guelcher SA, Srinivasan A, Dumas JE, Didier JE, McBride S, Hollinger JO. Synthesis, mechanical properties, biocompatibility, and biodegradation of polyurethane networks from lysine polyisocyanates. *Biomaterials* 2008;29(12):1762–75.
- Turner TM, Urban RM, Singh K, Hall DJ, Renner SM, Lim T-H, et al. Vertebroplasty comparing injectable calcium phosphate cement compared with polymethylmethacrylate in a unique canine vertebral body large defect model. *The Spine Journal* 2008;8(3):482–7.
- Link DP, van den Dolder J, van den Beucken JJ, Wolke JG, Mikos AG, Jansen JA. Bone response and mechanical strength of rabbit femoral defects filled with injectable CaP cements containing TGF- $\beta$ 1 loaded gelatin microparticles. *Biomaterials* 2008;29(6):675–82.
- Xu HHK, Weir MD, Burguera EF, Fraser AM. Injectable and macroporous calcium phosphate cement scaffold. *Biomaterials* 2006;27(24):4279–87.
- Elsner A, Jubel A, Prokop A, Koebke J, Rehm KE, Andermahr J. Augmentation of intra-articular calcaneal fractures with injectable calcium phosphate cement: densitometry, histology, and functional outcome of 18 patients. *The Journal of Foot and Ankle Surgery* 2005;44(5):390–5.
- Apelt D, Theiss F, El-Warrak AO, Zlinszky K, Bettschart-Wolfsberger R, Bohner M, et al. In vivo behavior of three different injectable hydraulic calcium phosphate cements. *Biomaterials* 2004;25(7–8):1439–51.
- Joosten U, Joist A, Frebel T, Brandt B, Diederichs S, von Eiff C. Evaluation of an in situ setting injectable calcium phosphate as a new carrier material for gentamicin in the treatment of chronic osteomyelitis: studies in vitro and in vivo. *Biomaterials* 2004;25(18):4287–95.
- Stanton DC, Chou JC, Carrasco LR. Injectable calcium-phosphate bone cement (Norian) for reconstruction of a large mandibular defect: a case report. *Journal of Oral and Maxillofacial Surgery* 2004;62(2):235–40.
- Ooms EM, Egglezos EA, Wolke JGC, Jansen JA. Soft-tissue response to injectable calcium phosphate cements. *Biomaterials* 2003;24(5):749–57.
- Horstmann WG, Verheyen CCPM, Leemans R. An injectable calcium phosphate cement as a bone-graft substitute in the treatment of displaced lateral tibial plateau fractures. *Injury* 2003;34(2):141–4.
- Daculsi G, Weiss P, Delecrin J, Grimandi G, Passuti N, Guerin F, inventors. Biomaterial composition and method for preparing same. Patent WO9521634; 1995.
- Daculsi G, Weiss P, Dupraz A, Lapkowski M, inventors. Biomaterial composition and method for preparing same. Patent WO9705911; 1997.
- Daculsi G, Weiss P, Bouler JM, Gauthier O, Millot F, Aguado E. Biphasic calcium phosphate/hydrolyzable polymer composites: a new concept for bone and dental substitution biomaterials. *Bone* 1999 Aug;25(2 Suppl.):59S–61S.
- Weiss P, Gauthier O, Bouler JM, Grimandi G, Daculsi G. Injectable bone substitute using a hydrophilic polymer. *Bone* 1999 Aug;25(2 Suppl.):67S–70S.
- Bourges X, Schmitt M, Amouriq Y, Daculsi G, Legeay G, Weiss P. Interaction between hydroxypropyl methylcellulose and biphasic calcium phosphate after steam sterilisation: capillary gas chromatography studies. *Journal of Biomaterials Science* 2001;12(6):573–9.
- Gauthier O, Goyenville E, Bouler JM, Guicheux J, Pilet P, Weiss P, et al. Macroporous biphasic calcium phosphate ceramics versus injectable bone substitute: a comparative study 3 and 8 weeks after implantation in rabbit bone. *Journal of Materials Science* 2001 May;12(5):385–90.
- Gauthier O, Khairoun I, Bosco J, Obadia L, Bourges X, Rau C, et al. Noninvasive bone replacement with a new injectable calcium phosphate biomaterial. *Journal of Biomedical Materials Research* 2003 July 1;66(1):47–54.
- Gauthier O, Muller R, von Stechow D, Lamy B, Weiss P, Bouler J-M, et al. In vivo bone regeneration with injectable calcium phosphate biomaterial: a three-dimensional micro-computed tomographic, biomechanical and SEM study. *Biomaterials* 2005;26(27):5444–53.
- Weiss P, Layrolle P, Clergeau LP, Enckel B, Pilet P, Amouriq Y, et al. The safety and efficacy of an injectable bone substitute in dental sockets demonstrated in a human clinical trial. *Biomaterials* 2007 Aug;28(22):3295–305.
- Bourges X, Weiss P, Daculsi G, Legeay G. Synthesis and general properties of silylated-hydroxypropyl methylcellulose in prospect of biomedical use. *Advances in Colloid and Interface Science* 2002;99(3):215–28.
- Bourges X, Weiss P, Coudreuse A, Daculsi G, Legeay G. General properties of silylated hydroxyethylcellulose for potential biomedical applications. *Biopolymers* 2002 Apr 5;63(4):232–8.
- Bourges X, Gauthier O, Grimandi G, Daculsi G, Legeay G, Weiss P. Développement d'un hydrogel autodurcissant in vivo, en perspective d'un usage biomédical. [A new self-hardening gel in prospect of biomedical use]. *ITBM-RBM* 2003;24(4):185–91.
- Fellah BH, Weiss P, Gauthier O, Rouillon T, Pilet P, Daculsi G, et al. Bone repair using a new injectable self-crosslinkable bone substitute. *Journal of Orthopaedic Research* 2006 Apr;24(4):628–35.
- Guicheux J, Vinatier C, Grimandi G, Daculsi G, Weiss P, inventors. INSERM, assignee. Brevet Innovation thérapeutique: Une matrice extracellulaire synthétique constituée d'un gel aqueux auto réticulant pour l'ingénierie tissulaire du cartilage. France patent 03292753.2; 2004 04-11-2003.
- Vinatier C, Guicheux J, Daculsi G, Layrolle P, Weiss P. Cartilage and bone tissue engineering using hydrogels. *Bio-Medical Materials and Engineering* 2006;16(4 Suppl.):S107–13.
- Trojani C, Weiss P, Michiels JF, Vinatier C, Guicheux J, Daculsi G, et al. Three-dimensional culture and differentiation of human osteogenic cells in an injectable hydroxypropylmethylcellulose hydrogel. *Biomaterials* 2005 Sep;26(27):5509–17.
- Vinatier C, Magne D, Moreau A, Gauthier O, Malard O, Vignes-Colombeix C, et al. Engineering cartilage with human nasal chondrocytes and a silanized hydroxypropyl methylcellulose hydrogel. *Journal of Biomedical Materials Research* 2007 Jan;80(1):66–74.
- Trojani C, Boukhechba F, Scimeca J-C, Vandebos F, Michiels J-F, Daculsi G, et al. Ectopic bone formation using an injectable biphasic calcium phosphate/Si-HPMC hydrogel composite loaded with undifferentiated bone marrow stromal cells. *Biomaterials* 2006;27(17):3256–64.
- Elabd C, Chiellini C, Massoudi A, Cochet O, Zaragosi L-E, Trojani C, et al. Human adipose tissue-derived multipotent stem cells differentiate in vitro and in vivo into osteocyte-like cells. *Biochemical and Biophysical Research Communications* 2007;361(2):342–8.
- Yamada S, Heymann D, Bouler JM, Daculsi G. Osteoclastic resorption of calcium phosphate ceramics with different hydroxyapatite/[beta]-tricalcium phosphate ratios. *Biomaterials* 1997;18(15):1037–41.
- Laib S, Petit M, Bodio E, Fatimi A, Weiss P, Bujoli B. Labeling of a self-hardening bone substitute using ruthenium tris-bipyridine complexes, for the analysis of its in vivo metabolism. *Comptes Rendus Chimie* 2008;11(6–7):641–9.
- Bouler JM, LeGeros RZ, Daculsi G. Biphasic calcium phosphates: influence of three synthesis parameters on the HA/beta-TCP ratio. *Journal of Biomedical Materials Research* 2000 Sep 15;51(4):680–4.
- Fatimi A, Tassin JF, Axelos MAV, Weiss P. Sedimentation study of biphasic calcium phosphate particles. *Key Engineering Materials* 2008;365–8.
- Fatimi A, Tassin JF, Quillard S, Axelos MAV, Weiss P. The rheological properties of silylated hydroxypropylmethylcellulose tissue engineering matrices. *Biomaterials* 2008;29(5):533–43.
- Mengshol JA, Vincenti MP, Brinckerhoff CE. IL-1 induces collagenase-3 (MMP-13) promoter activity in stably transfected chondrocytic cells: requirement for Runx-2 and activation by p38 MAPK and JNK pathways. *Nucleic Acids Research* 2001 Nov 1;29(21):4361–72.
- Magne D, Bluteau G, Fauchoux C, Palmer G, Vignes-Colombeix C, Pilet P, et al. Phosphate is a specific signal for ATDC5 chondrocyte maturation and apoptosis-associated mineralization: possible implication of apoptosis in the regulation of endochondral ossification. *Journal of Bone Mineral Research* 2003 Aug;18(8):1430–42.
- Relic B, Guicheux J, Mezin F, Lubberts E, Togninalli D, Garcia I, et al. IL-4 and IL-13, but not IL-10, protect human synoviocytes from apoptosis. *Journal of Immunology* 2001 Feb 15;166(4):2775–82.
- Kimura H, Sugaya K, Cook PR. The transcription cycle of RNA polymerase II in living cells. *The Journal of Cell Biology* 2002 Dec 9;159(5):777–82.
- Hollinger JO, Kleinschmidt JC. The critical size defect as an experimental model to test bone repair materials. *The Journal of Craniofacial Surgery* 1990 Jan;1(1):60–8.
- Movat HZ. Demonstration of all connective tissue elements in a single section; pentachrome stains. A. M. A. *Archives of Pathology* 1955 Sep;60(3):289–95.
- Russell Jr HK. A modification of Movat's pentachrome stain. *Archives of Pathology* 1972 Aug;94(2):187–91.
- Vinatier C, Magne D, Weiss P, Trojani C, Rochet N, Carle GF, et al. A silanized hydroxypropyl methylcellulose hydrogel for the three-dimensional culture of chondrocytes. *Biomaterials* 2005 Nov;26(33):6643–51.
- Bui P, Pons-Guiraud A, Kuffer R, Plantier F, Nicolau P. Les produits injectables lentement et non résorbables. *Annales De Chirurgie Plastique Esthétique* 2004;49(5):486–502.